

铒镱共掺光纤制备及其激光性能研究

陈阳, 褚应波, 戴能利, 李进延*

华中科技大学武汉光电国家研究中心, 湖北 武汉 430074

摘要 铒镱($\text{Er}^{3+}/\text{Yb}^{3+}$)共掺光纤是实现波长为 $1.5\ \mu\text{m}$ 激光的重要增益介质之一。但是石英基 $\text{Er}^{3+}/\text{Yb}^{3+}$ 共掺光纤很容易产生波长为 $1\ \mu\text{m}$ 的放大的自发辐射(ASE)光, 不仅降低 $1.5\ \mu\text{m}$ 激光的泵浦转换效率, 而且是限制 $1.5\ \mu\text{m}$ 激光功率提升的“瓶颈”。研究结果表明, 提升纤芯磷的掺杂量, 能够增大纤芯基质的最大声子能量, 有利于抑制 Yb^{3+} 的 ASE 光和 $\text{Er}^{3+} \rightarrow \text{Yb}^{3+}$ 的反向能量传递, 从而提高 $\text{Er}^{3+}/\text{Yb}^{3+}$ 共掺光纤的泵浦转换效率。通过改良的化学气相沉积制备工艺可以减少磷元素在高温条件下的挥发, 从而成功制备出高掺磷的 $10/130\ \mu\text{m}$ 双层包层 $\text{Er}^{3+}/\text{Yb}^{3+}$ 共掺光纤。测试光纤后向的 $1\ \mu\text{m}$ ASE 光谱随泵浦功率的变化, 并且搭建两级激光测试平台, 测得 $\text{Er}^{3+}/\text{Yb}^{3+}$ 共掺光纤激光的斜率效率为 35.5%。

关键词 激光光学; 铒镱共掺光纤; $1.5\ \mu\text{m}$ 激光; 光纤激光器; 改良的化学气相沉积

中图分类号 O436

文献标志码 A

doi: 10.3788/CJL202148.0701007

1 引言

波长为 $1.5\ \mu\text{m}$ 激光位于石英光纤的低损耗传输窗口, 具有“人眼安全”的重要特性, 在通信、医学、激光雷达、军工和科研等领域得到了广泛的应用^[1-4]。科研人员对掺 Er^{3+} ^[5] 或 $\text{Er}^{3+}/\text{Yb}^{3+}$ 共掺材料进行了广泛研究, $\text{Er}^{3+}/\text{Yb}^{3+}$ 共掺光纤是产生 $1.5\ \mu\text{m}$ 激光的重要增益介质之一, 所以备受研究者的关注。 Yb^{3+} 在 $800\sim 1100\ \text{nm}$ 波段有很宽的吸收带^[6], 在波长为 $980\ \text{nm}$ 处的吸收峰强度是 Er^{3+} 的十几倍。同时, Yb^{3+} 的发射谱与 Er^{3+} 的吸收谱有较大范围的重叠。当离子间距足够近时, Yb^{3+} 与 Er^{3+} 之间发生共振能量传递, 有利于提高 Er^{3+} 的 $1.5\ \mu\text{m}$ 发光效率。与此同时, Yb^{3+} 在石英玻璃中的溶解度更大, 引入 Yb^{3+} 有利于增大 Er^{3+} 间距, 能够有效减少 Er^{3+} 的团簇效应^[7]。但是, 当 Yb^{3+} 的泵浦速率大于 $\text{Yb}^{3+} \rightarrow \text{Er}^{3+}$ 的能量传递速率时, Yb^{3+} 的 $^2\text{F}_{5/2}$ 能级会积累大量的激活粒子, 使 $1\ \mu\text{m}$ 信号因出现不饱和增益^[8] 而在激光器系统中逐渐被放大, 这不仅会降低系统的泵浦转化效率, 还可能产生寄生激光甚至巨脉冲, 从而烧坏光纤的输出端面。

波长为 $1\ \mu\text{m}$ 自发辐射(ASE)光是制约 $\text{Er}^{3+}/\text{Yb}^{3+}$ 共掺光纤激光器的转换效率, 以及输出功率提升的关键因素之一^[9-10], 抑制 Yb^{3+} 的 $1\ \mu\text{m}$ ASE 光成为研究 $\text{Er}^{3+}/\text{Yb}^{3+}$ 共掺光纤激光器的重要课题之一。目前, 抑制波长为 $1\ \mu\text{m}$ ASE 光的方案主要包括改进激光器系统、设计光纤结构和调整纤芯组分三种。改进光纤激光器系统主要采用非峰值泵浦来降低泵浦速率, 或引入辅助种子源^[8, 11]、环形腔^[12] 和光栅^[13], 从而避免 $1\ \mu\text{m}$ ASE 光的积累; 微结构光纤具有十分灵活的结构设计^[14], 通过调整光纤结构可以使 $1\ \mu\text{m}$ ASE 光的损耗大大增加, 从而避免 $1\ \mu\text{m}$ ASE 光的积累^[15-16]; 调整光纤组分, 主要是提高纤芯磷(P)元素的掺杂量, 从而抑制 $\text{Er}^{3+} \rightarrow \text{Yb}^{3+}$ 的反向能量传递效率^[17], 并缩短 Yb^{3+} 的 $^2\text{F}_{5/2}$ 能级寿命。基于改进的化学气相沉积(MCVD)法在光纤材料层面抑制 $1\ \mu\text{m}$ ASE 光, 这对激光器系统的改变非常小, 无疑会节约光源设备和大量的光纤器件, 为实现 $1.5\ \mu\text{m}$ 高功率激光打下材料基础。

据报道, 基于 MCVD 法制备的 $\text{SiO}_2\text{-GeO}_2$ 体系光纤, 铒镱的能量传递效率仅有 5%^[18], 而磷酸盐玻璃中 $\text{Yb}^{3+} \rightarrow \text{Er}^{3+}$ 的能量传递效率高达 95%^[19],

收稿日期: 2020-09-04; 修回日期: 2020-09-23; 录用日期: 2020-11-1

基金项目: 国家自然科学基金青年科学基金(61805093)、中国博士后科学基金(2017M612450)

*E-mail: ljj@hust.edu.cn

增加石英光纤纤芯中的 P 含量,能够明显提高 $\text{Yb}^{3+} \rightarrow \text{Er}^{3+}$ 的能量传递效率^[20]。本文基于 MCVD 掺杂工艺与溶液掺杂技术并采用“反向沉积”的方式,实现纤芯中 P 元素的高掺杂,使用波长为 975 nm 的半导体激光器(LD)激发并监测波长为 1080 nm 的 ASE 光功率变化,当泵浦功率增大到 6.88 W 时,1080 nm ASE 光功率仍比 1.5 μm 激光功率低约 58 dB。泵浦波长更换为 940 nm 的 LD 来测试 1550 nm 激光,其斜率效率可达 35.5%,输出功率为 2.5 W。

2 实验

$\text{Er}^{3+}/\text{Yb}^{3+}$ 共掺光纤预制棒是在课题组成熟的 MCVD 工艺的基础上完成。通过溶液浸泡的方式掺杂 Er^{3+} 和 Yb^{3+} ^[21],选择“反向沉积”工艺沉积 P 元素,可以减少其在制备过程中的挥发^[22]。其原因在于 MCVD 工艺的原理是“热泳”效应,反应料在高温区发生化学反应并在温度下游沉积,而 P_2O_5 的熔点仅有 340 $^{\circ}\text{C}$,升华温度仅有 360 $^{\circ}\text{C}$ ^[23],远低于 MCVD 工艺的沉积温度。“正向沉积”的工艺是指沉积物在火焰下方受到氢氧焰的二次加热,这会引入 P 元素严重挥发。P 元素的挥发在预制棒的折射率剖面上表现为中心下陷,研究结果表明 P 元素的挥发还会引起稀土元素的损失^[22]。最后,光纤拉丝在特种光纤拉丝塔上以 100 m/min 的速度拉制完成^[24]。

对于光纤预制棒,使用 Photon Kinetics 公司生产的光纤预制棒分析仪(P104)来表征芯子的折射率分布,成品光纤使用 Photon Kinetics 公司生产的光纤分析系统(PK2500)来表征,分别采用“截断法”和“替代法”^[25]来测试背景损耗和 850~1650 nm 波段的吸收谱。为了验证光纤的放大性能,分别搭建单级和两级放大测试平台,其中单级放大系统主要验证不同泵浦条件下波长为 1.55 μm 激光与 1 μm ASE 光的光谱变化情况,两级放大系统进一步优化测试激光系统的斜率效率。

3 实验结果与讨论

3.1 $\text{Er}^{3+}/\text{Yb}^{3+}$ 能级示意图

使用 915~980 nm 波段的泵浦 $\text{Er}^{3+}/\text{Yb}^{3+}$ 共掺光纤来放大 1.55 μm 激光的简易能级,如图 1 所示,主要能量交换过程如下。基态吸收(GSA)过程指 Yb^{3+} ($^2\text{F}_{7/2}$)能级吸收泵浦光子后被激发到 Yb^{3+} ($^2\text{F}_{5/2}$)能级。共振能量传递(ET)过程是指 $^2\text{F}_{5/2}$ 能

级将能量传递给基态 Er^{3+} , Er^{3+} 跃迁到上能级 $^4\text{I}_{11/2}$,而 Yb^{3+} 回落到基态能级。多声子辅助跃迁(MPR)过程是指 $^4\text{I}_{11/2}$ 能级的寿命约有 1 ns,在多个声子的辅助下迅速以无辐射跃迁的形式快速弛豫到 $^4\text{I}_{13/2}$ 能级。受激辐射(Radiation)过程是指 $^4\text{I}_{13/2}$ 能级的寿命较长,石英光纤中往往能够达到 7~10 ms,这会在 $^4\text{I}_{13/2}$ 与 $^4\text{I}_{11/2}$ 能级间形成粒子数反转分布。当有波长为 1.5 μm 的信号光注入时,就发生受激辐射(Radiation)过程,发射一个与信号光同波长的光子。激发态吸收(ESA)过程是指 $^4\text{I}_{13/2}$ 能级的寿命较长,当泵浦波长约为 980 nm 时,则会有较大几率吸收一个泵浦光子后跃迁到 $^4\text{F}_{9/2}$ 。但是由于基质材料的声子能量较大, $^4\text{F}_{9/2}$ 能级的离子会以多声子弛豫的形式回落到 $^4\text{I}_{13/2}$ 能级,这一过程会降低波长为 1.5 μm 的信号发光泵浦转换效率。

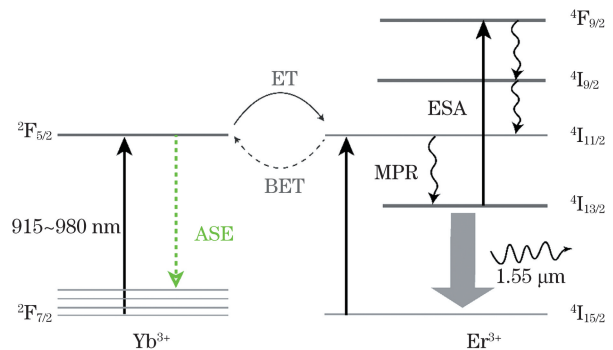


图 1 $\text{Er}^{3+}/\text{Yb}^{3+}$ 共掺光纤的能级示意图

Fig. 1 Energy level diagram of $\text{Er}^{3+}/\text{Yb}^{3+}$ co-doped fiber

3.2 光纤预制棒的制备与测试

使用 P104 光纤预制棒分析仪来分析光纤预制棒的折射率剖面,如图 2 所示。从图 2 可以看到,数值孔径(NA)为 0.216,预制棒的芯径为 2.66 mm,中心凹陷是成棒过程中纤芯 P 元素挥发的表现。预制棒拉丝是在特种光纤拉丝塔中以 1980 $^{\circ}\text{C}$ 高温

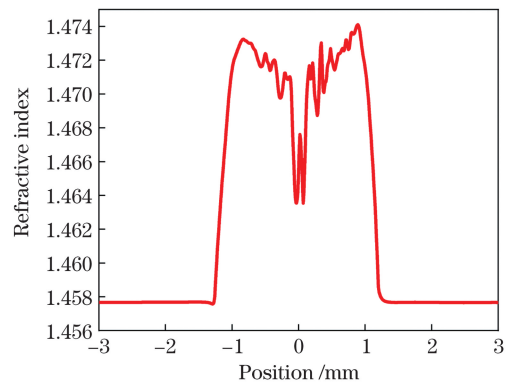


图 2 光纤预制棒的折射率剖面

Fig. 2 Refractive index profile of optical fiber preform

进行的,控制拉丝速度将预制棒拉制成外径为 $130\ \mu\text{m}$ 的双包层光纤,光纤纤芯的直径为 $10\ \mu\text{m}$ 。光纤背景损耗与包层吸收系数分别采用“截断法”和“替代法”进行测试^[22],测试结果如图 3 所示。从

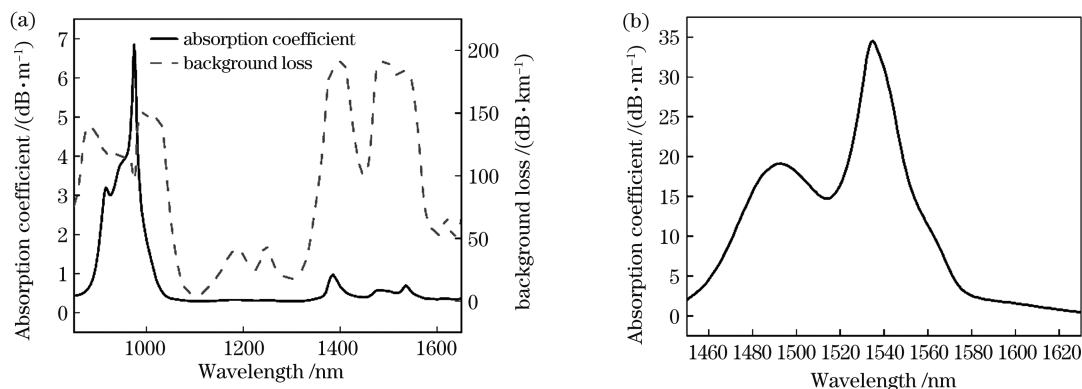


图 3 吸收系数与背景损耗的变化曲线。(a)包层吸收系数与背景损耗;(b)纤芯吸收系数

Fig. 3 Change curves of absorption coefficient and background loss. (a) Cladding absorption coefficient and background loss; (b) core absorption coefficient

3.3 $1\ \mu\text{m}$ ASE 光纤的光谱测试

图 4 为激光放大测试平台,由种子光、波分复用器(WDM)、合束器(Combiner)、隔离器和滤波器等构成,其中 EYDF 为共掺双包层光纤。型号为 TSL-550 的可调谐激光器提供种子光,中心波长设为 $1549.96\ \text{nm}$,种子光经过光纤隔离器(ISO)后进入系统中。 $1060/1550\ \text{WDM}$ 将种子光耦合进 $5.5\ \text{m}$ 长的有源光纤中,同时将 $1\ \mu\text{m}$ ASE 光导出并传输进光谱仪中。由于 $1\ \mu\text{m}$ ASE 光功率较低,ASE 光

图 3(a)可以看到,测得背景损耗在 $1190\ \text{nm}$ 的波长处为 $42.15\ \text{dB/km}$,包层吸收系数在 $940\ \text{nm}$ 的波长处为 $3.58\ \text{dB/m}$ 。从图 3(b)可以看到,纤芯吸收系数在 $1535\ \text{nm}$ 的波长处为 $34.5\ \text{dB/m}$ 。

谱和功率均由光谱仪获得。将波长为 $976\ \text{nm}$ 的 LD 作为泵浦光源,光源经过合束器耦合后进入钕镱光纤中并进行反向泵浦。放大后的激光先后经过 ISO 和滤波器,其中 ISO 1 用于避免背向反射光干扰种子光源的输出,而 ISO 2 则用于避免由光纤输出端面回光反射造成激光器的输出功率不稳定,滤波器用于滤除波长为 $1550\ \text{nm}$ 两侧的 ASE 光,从而保证功率测试结果更准确。

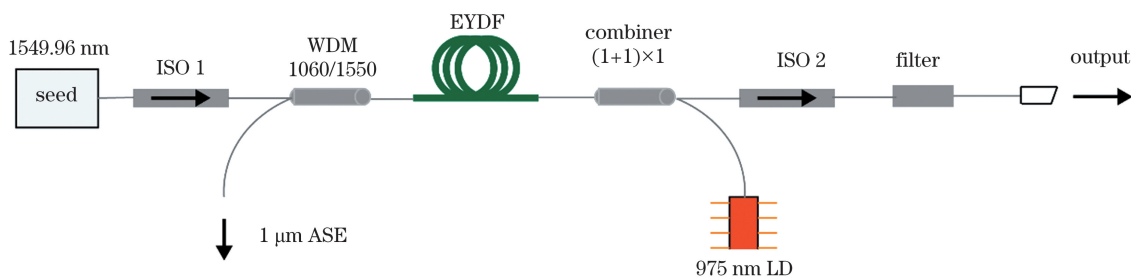


图 4 ASE 测试结构图

Fig. 4 ASE test structure chart

Yb^{3+} 位于 $1000\sim 1150\ \text{nm}$ 波段的后向 ASE 光谱随泵浦功率变化的曲线,如图 5 所示,插图对应波长为 $1550\ \text{nm}$ 激光的输出功率变化曲线。从图 5 可以看到,在泵浦功率逐渐增加的过程中, $1.5\ \mu\text{m}$ 激光功率持续增加,斜率效率达到 30% ;ASE 光的功率虽然不断增大,但是峰值功率仍低于 $-45\ \text{dBm}$;ASE 光并没有随着泵浦光功率的增大迅速积累,其原因可能与掺 P 元素提高了 $\text{Yb}^{3+} \rightarrow \text{Er}^{3+}$ 的能量传递效率有关。P 元素在 SiO_2 网络中

形成四面体单元,但是形成 P=O 双键。P=O 双键的拉曼峰位于 $1330\ \text{cm}^{-1}$ 附近,这会增大玻璃材料的最大声子能量。当 Er^{3+} 占据 P=O 的附近位点时,P=O 与 Er^{3+} 发生强烈共振,从而促进 ${}^4\text{I}_{11/2}$ 能级的粒子快速无辐射弛豫到下一能级, ${}^4\text{I}_{11/2}$ 能级的粒子数迅速减少,减小 $\text{Er}^{3+} \rightarrow \text{Yb}^{3+}$ 的反向能量传递几率。多声子弛豫几率可以表示为

$$N = N_0 \exp(-\alpha \Delta E / h\omega_p) = N_0 \exp(-\alpha P), \quad (1)$$

式中: N 为多声子弛豫几率; N_0 为绝对零度下能级

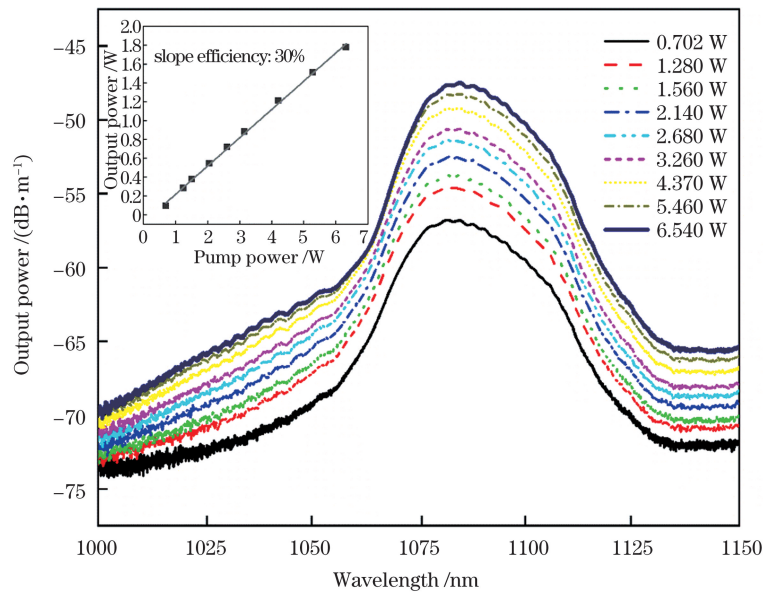


图 5 波长为 1.55 μm 的激光输出功率随泵浦功率变化的曲线

Fig. 5 Curves of laser output power of 1.55 μm with pump power

差为 0 的弛豫几率; h 为普朗克常数; ΔE 为发生多声子弛豫过程的两能级差; P 为发生弛豫的声子级数; ω_p 为系统最大振动频率; α 为与基质材料相关的常量。由(1)式可以看到, 多声子弛豫几率与声子能量成 e 指数关系。Er³⁺/Yb³⁺ 共掺系统, Yb³⁺ 的能级寿命可以表示为^[26]

$$k = k_{Yb} + k_{ET} [Er^{3+}]^x, \quad (2)$$

式中: $k = 1/\tau$, τ 为测试得到的 Yb³⁺ 荧光寿命; k_{Yb} 为 Yb³⁺ 的衰减常数; k_{ET} 为 Yb³⁺ 向 Er³⁺ 的能量传递速率; $[Er^{3+}]$ 为 Er³⁺ 的浓度; x 为依赖能量传递机制的常数。Er³⁺ 能级寿命^[27]可以表示

$$\tau_{Er} = \frac{1}{\Gamma_R + \Gamma_{NR}}, \quad (3)$$

式中: τ_{Er} 为 Er³⁺ 的 ⁴I_{13/2} 能级寿命; Γ_R 为辐射衰减速率; Γ_{NR} 为非辐射衰减速率。基质最大声子能量的增加, 不仅会降低钇离子的能级寿命, 促进 Yb³⁺ → Er³⁺ 能量传递, 还会间接减少 Yb³⁺ 的能级寿命。

3.4 光纤激光性能测试

为了进一步验证自制 Er³⁺/Yb³⁺ 共掺光纤的激

光性能, 搭建图 6 的两级激光测试平台, 其中 EDF 为掺铒光纤。第一级主要用于对信号光进行预放大, 其熔接长为 8 m 的钇纤, 使用波长为 980 nm 单模前向泵浦作为泵浦源。第二级熔接 Er³⁺/Yb³⁺ 共掺光纤, 测试激光的放大性能。种子光与泵浦光通过一支 980/1550 WDM 耦合后进入一级钇纤中。为了阻挡后一级背向传输光对上一级种子光或放大级造成的影响, 在种子光的输出端、两级放大结构之间以及激光器的输出端, 各熔接一支 ISO。两级放大结构的中间熔接一支窄带滤波器, 用于滤除第一级产生的 ASE 光。第二级放大结构中将带尾纤的多模 940 nm 的 LD 作为泵浦源, 通过一支 (1+1) × 1 合束器后反向耦合进光纤中。激光放大测试过程中, 截取 5.5 m 长的光纤熔接到测试系统二级结构中, 注入种子光的平均波长为 1554.91 nm, 信号功率为 -0.086 dBm。测试二级各泵浦功率下的激光输出功率, 并将所得数据进行线性拟合, 结果如图 7 所示。从图 7 可以看到, 斜率效率为 35.5%, 相关系数 $R^2 = 0.99805$; 当输出功率达到 2.5 W 时, 效

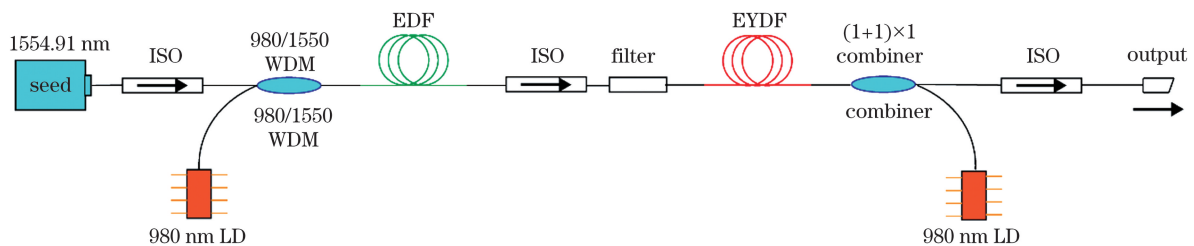


图 6 激光测试装置图

Fig. 6 Laser performance test experimental setup

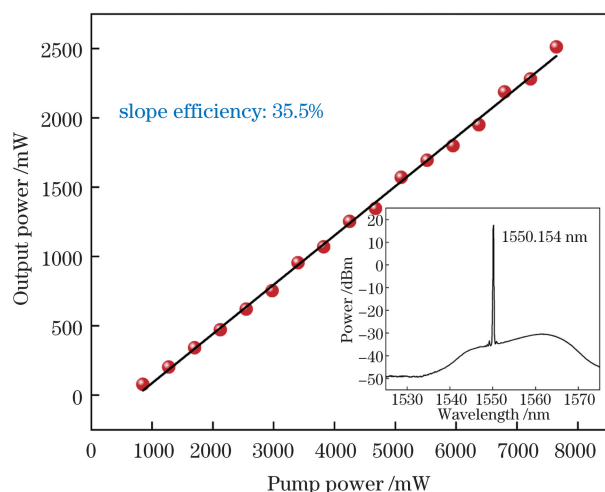


图 7 波长为 1550 nm 的激光输出功率随泵浦功率变化曲线及其输出功率最大时的输出光谱

Fig. 7 Output power of laser with wavelength of 1550 nm varies with pump power and output spectrum when output power is maximum

率仍未出现下降,说明此时 $1 \mu\text{m}$ ASE 光并未影响到 $1.5 \mu\text{m}$ 激光的输出。将输出光纤连接一支衰减器后耦合进光谱仪中,测试激光与 $1.5 \mu\text{m}$ ASE 光谱,如图 7 插图所示。从图 7 插图可以看到,当激光输出功率为 5 W 时,光谱地信噪比超过 50 dB。

4 结 论

基于 MCVD 工艺并结合溶液掺杂法,采用反向掺 P 成功制备出双包层 $\text{Er}^{3+}/\text{Yb}^{3+}$ 共掺光纤。光纤纤芯的直径为 $10 \mu\text{m}$,包层直径为 $130 \mu\text{m}$,包层吸收系数在 940 nm 的波长处为 3.58 dB/m ,纤芯吸收系数在 1535 nm 的波长处为 34.5 dB/m 。激光测试结果表明,高掺 P 可以有效抑制 $1 \mu\text{m}$ ASE 光,波长为 $1.5 \mu\text{m}$ 激光的斜率效率最大可达 35.5% ,输出功率为 2.5 W 。该 $\text{Er}^{3+}/\text{Yb}^{3+}$ 共掺光纤的成功研制为进一步研究 $1.5 \mu\text{m}$ 高功率光纤激光器打下坚实的基础。

参 考 文 献

- [1] Cheng Y S, Chen G, Li J Y. Research progress of high-power erbium-ytterbium codoped fiber laser[J]. Laser & Optoelectronics Progress, 2019, 56(17): 170607.
程永师, 陈瑰, 李进延. 高功率铒镱共掺光纤激光器研究进展[J]. 激光与光电子学进展, 2019, 56(17): 170607.
- [2] Diaz J C F, Carter W E, Shrestha R L, et al. LiDAR remote sensing [M] // Handbook of Satellite

Applications. Cham: Springer, 2017: 929-980.

- [3] Li B, Tong S F, Zhang L, et al. Influence of horizontal atmospheric visibility on deep-space laser communication rate[J]. Acta Optica Sinica, 2017, 37(10): 1006003.
李勃, 佟首峰, 张雷, 等. 水平大气能见度对深空激光通信速率的影响[J]. 光学学报, 2017, 37(10): 1006003.
- [4] Zhang K L, Chen H W, Lu B L, et al. Passively Q-switched erbium-doped fiber laser based on HfSe_2 saturable absorber[J]. Acta Optica Sinica, 2020, 40(13): 1314001.
张凯龙, 陈浩伟, 陆宝乐, 等. 基于二硒化铪可饱和吸收体的被动调 Q 掺铒光纤激光器的研究[J]. 光学学报, 2020, 40(13): 1314001.
- [5] Chen Y J, Lin Y F, Huang J H, et al. Research progress in 1550-nm all-solid-state lasers based on Er^{3+} -doped crystals[J]. Chinese Journal of Lasers, 2020, 47(5): 0500018.
陈雨金, 林炎富, 黄建华, 等. 基于掺 Er^{3+} 晶体的 1550 nm 波段全固态激光研究进展[J]. 中国激光, 2020, 47(5): 0500018.
- [6] Vienne G. Fabrication and characterisation of ytterbium:erbium codoped phosphosilicate fibres for optical amplifiers and lasers [D]. Southampton: University of Southampton, 1997.
- [7] Codemard C, Soh D B S, Ylä-Jarkko K, et al. Cladding-pumped L-band phosphosilicate erbium-ytterbium co-doped fiber amplifier [C] // Optical Amplifiers and Their Applications, July 6-9, 2003, Otaru, Japan. Washington, D. C.: OSA, 2003: TuC2.
- [8] Kuhn V, Weßels P, Neumann J, et al. Stabilization and power scaling of cladding pumped $\text{Er} : \text{Yb}$ -codoped fiber amplifier via auxiliary signal at 1064 nm [J]. Optics Express, 2009, 17(20): 18304-18311.
- [9] Han Q, Yao Y Z, Chen Y F, et al. Highly efficient Er/Yb -codoped fiber amplifier with an Yb -band fiber Bragg grating [J]. Optics Letters, 2015, 40(11): 2634-2636.
- [10] Dong L, Matniyaz T, Kalichevsky-Dong M T, et al. Modeling Er/Yb fiber lasers at high powers [J]. Optics Express, 2020, 28(11): 16244-16255.
- [11] Kuhn V, Kracht D, Neumann J, et al. Dependence of $\text{ErH} : \text{Yb}$ -codoped $1.5 \mu\text{m}$ amplifier on wavelength-tuned auxiliary seed signal at $1 \mu\text{m}$ wavelength [J]. Optics Letters, 2010, 35(24): 4105-4107.
- [12] Sobon G, Sliwinska D, Abramski K M, et al. 10 W single-mode Er/Yb co-doped all-fiber amplifier with suppressed Yb -ASE [J]. Laser Physics Letters,

- 2014, 11(2): 025103.
- [13] Han Q, Yan W C, Yao Y Z, et al. Optimal design of Er/Yb co-doped fiber amplifiers with an Yb-band fiber Bragg grating[J]. *Photonics Research*, 2016, 4(2): 53-56.
- [14] Hu X W. Research on fabrication technology and sensing property of novel photonic crystal fiber[D]. Wuhan: Huazhong University of Science and Technology, 2018.
胡雄伟. 新型光子晶体光纤的制备技术与传感特性研究[D]. 武汉: 华中科技大学, 2018.
- [15] Shirakawa A, Suzuki H, Tanisho M, et al. Yb-ASE-free Er amplification in short-wavelength filtered Er:Yb photonic-crystal fiber [C] // OFC/NFOEC 2008-2008 Conference on Optical Fiber Communication/National Fiber Optic Engineers Conference, February 24-28, 2008, San Diego, CA, USA. New York: IEEE, 2008: 1-3.
- [16] Ouyang D Q, Guo C Y, Ruan S C, et al. Yb band parasitic lasing suppression in Er/Yb-co-doped pulsed fiber amplifier based on all-solid photonic bandgap fiber[J]. *Applied Physics B*, 2014, 114(4): 585-590.
- [17] Tankala K, Samson B, Carter A, et al. New developments in high power eye-safe LMA fibers[J]. *Proceedings of SPIE*, 2006, 6102: 610206.
- [18] Grubb S G, Cannon R S, Windhorn T W, et al. High-power sensitized erbium optical fiber amplifier [C] // Optical Fiber Communication, February 18, 1991, San Diego, California. Washington, D. C.: OSA, 1991: PD7.
- [19] Hwang B C, Jiang S B, Luo T, et al. Cooperative upconversion and energy transfer of new high Er³⁺- and Yb³⁺-Er³⁺-doped phosphate glasses[J]. *Journal of the Optical Society of America B*, 2000, 17(5): 833-839.
- [20] Zhang Z X, Jiang Z W, Peng J G, et al. Fabrication and characterization of Er³⁺:Yb³⁺ co-doped phosphosilicate fibers [J]. *Journal of Inorganic Materials*, 2012, 27(5): 485-488.
张泽学, 蒋作文, 彭景刚, 等. 钇镱共掺磷硅酸盐光纤的制备及其激光性能研究[J]. *无机材料学报*, 2012, 27(5): 485-488.
- [21] Townsend J E, Poole S B, Payne D N. Solution-doping technique for fabrication of rare-earth-doped optical fibres[J]. *Electronics Letters*, 1987, 23(7): 329.
- [22] Abramov A N, Bubnov M M, Vechkanov N N, et al. Fabrication of heavily Er₂O₃ doped aluminophosphosilicate glass fibers [J]. *Inorganic Materials*, 2010, 46(4): 439-444.
- [23] Gao C, Huang Z H, Wang Y Y, et al. Yb-doped aluminophosphosilicate laser fiber [J]. *Journal of Lightwave Technology*, 2016, 34(22): 5170-5174.
- [24] Snitzer E, Po H, Hakimi F, et al. Double clad, offset core Nd fiber laser [C] // Optical Fiber Sensors 1988, January 27, 1988, New Orleans, Louisiana United States. Washington, D.C.: OSA, 1988: PD5.
- [25] Li H Q, Liu C P, Zhao N, et al. Study on the absorption coefficient measurement of Yb-doped fiber [J]. *Optics & Optoelectronic Technology*, 2017, 15(1): 72-75.
李海清, 刘超平, 赵楠, 等. 掺镱光纤的吸收系数测试研究[J]. *光学与光电技术*, 2017, 15(1): 72-75.
- [26] Wu R K, Myers J D, Myers M J, et al. Fluorescence lifetime and 980-nm pump energy transfer dynamics in erbium and ytterbium co-doped phosphate laser glasses[J]. *Proceedings of SPIE*, 2003, 4968: 11-17.
- [27] Zhang J X J, Hoshino K. Optical transducers: optical molecular sensing and spectroscopy [M] // *Molecular Sensors and Nanodevices*. Amsterdam: Elsevier, 2019: 231-309.

Fabrication of Erbium-Ytterbium Co-Doped Fiber and Fiber Laser Performance Study

Chen Yang, Chu Yingbo, Dai Nengli, Li Jinyan*

Wuhan National Laboratory for Optoelectronics, Huazhong University of Science and Technology,
Wuhan, Hubei 430074, China

Abstract

Objective Er³⁺/Yb³⁺ co-doped fiber laser has attracted significant attention. It is widely applied in communication, military, medical, and scientific research fields. Er³⁺/Yb³⁺ co-doped fiber laser operates at 1.5 μm, which is located in the low-loss transmission window of silica fiber and considered as an eye-safe wavelength band. In Er³⁺/Yb³⁺ co-doped fiber, Yb³⁺ ions, which act as an excellent sensitizer, have wide absorption bands of 800–1000 nm and high

absorption intensity. When Yb^{3+} and Er^{3+} are sufficiently close, resonance energy transfer occurs between them, which improve the luminescence efficiency at $1.5\ \mu\text{m}$. The introduction of Yb^{3+} also increases the distance between Er^{3+} and prevents Er^{3+} from forming clusters. However, the amplified spontaneous emission (ASE) at $1\ \mu\text{m}$ emitted by Yb^{3+} is inclined to give rise to the bottleneck effect of $\text{Er}^{3+}/\text{Yb}^{3+}$ co-doped fiber lasers. The output power of $1.5\text{-}\mu\text{m}$ laser and the slope efficiency will be strongly diminished by the ASE of Yb^{3+} . In this study, a series of technical solutions to alleviate ASE is proposed to achieve high efficiency $\text{Er}^{3+}/\text{Yb}^{3+}$ co-doped fiber lasers. Most of the proposed methods focus on changing the structure of fiber lasers. However, optimizing the composition of the fiber core and fabricating high-performance $\text{Er}^{3+}/\text{Yb}^{3+}$ co-doped fiber seems to be a more fundamental approach to suppress ASE. Thus, the $\text{Er}^{3+}/\text{Yb}^{3+}$ co-doped fiber is prepared by modified chemical vapor deposition (MCVD) process combined with solution doping technology, and the $\text{Er}^{3+}/\text{Yb}^{3+}$ co-doped fiber laser system is constructed. Finally, the output power and ASE spectra at different pump powers are investigated.

Methods The MCVD and solution doping technologies are used to prepare fibers by introducing a large amount of phosphorus into the core. The refractive index profile (RIP) of the fiber is also analyzed by P104. Moreover, PK2500 is utilized to test the background loss and absorption coefficient of the fiber. The ASE test structure, as shown in Fig. 4, is established to observe a $1\text{-}\mu\text{m}$ ASE spectrum, which varies with pump power. The linear relationship between the output power of the 1550-nm laser and the pump power is also observed. The laser test configuration, as shown in Fig. 6, is established to further verify the fiber laser performance. By optimizing the fiber, the slope efficiency and output power are 35.5% and $2.5\ \text{W}$, respectively.

Results and Discussions Fig. 2 shows the RIP of the optical fiber preform. The numerical aperture (NA) attains 0.216 , and the RIP center depression is caused by the volatilization of the core phosphorus element during the collapsing process. Fig. 3 shows related optical fiber performance parameters. The background loss is about $42.15\ \text{dB/km}$ at $1190\ \text{nm}$. The cladding absorption coefficient at $940\ \text{nm}$ and the core absorption coefficient at $1535\ \text{nm}$ are $3.58\ \text{dB/m}$ and $34.5\ \text{dB/m}$, respectively. The backward $1\text{-}\mu\text{m}$ ASE spectrum changes with the pump source power, as shown in Fig. 5. The inset shows that the $1.5\text{-}\mu\text{m}$ laser power increases in synchronization. When the Yb^{3+} pumping rate is faster than the energy transfer rate of $\text{Yb}^{3+} \rightarrow \text{Er}^{3+}$, the ${}^2\text{F}_{5/2}$ energy level of Yb^{3+} will accumulate a large number of the excited state particles, and the $1\text{-}\mu\text{m}$ signal will gradually be amplified in the laser system due to the unsaturated gain. Thus, it reduces the system pump conversion efficiency and produces parasitic lasers or even giant pulses, which can burn the fiber output end face. For this fiber, along with the $1\text{-}\mu\text{m}$ ASE power continuing to increase, the peak power is below $-45\ \text{dBm}$ from beginning to end. The $1\text{-}\mu\text{m}$ ASE does not accumulate rapidly with the increase of pump light power. The reason may be attributed to the enhancement of $\text{Yb}^{3+} \rightarrow \text{Er}^{3+}$ energy transfer efficiency by phosphorus doping. A two-level laser test platform, as shown in Fig. 6, is developed to further verify the laser performance of the homemade $\text{Er}^{3+}/\text{Yb}^{3+}$ co-doped fiber. Furthermore, the laser output power under each pump power of the second stage is tested, and a linear fit is made to the obtained data. Fig. 7 shows the test result with a slope efficiency of 35.5% and coefficient of association of 0.99805 . When the output power reaches $2.5\ \text{W}$, there is still no over-rolling phenomenon, suggesting that the $1\text{-}\mu\text{m}$ ASE has no significant adverse impact on the $1.5\text{-}\mu\text{m}$ laser output.

Conclusions The $\text{Er}^{3+}/\text{Yb}^{3+}$ co-doped double-clad fiber is successfully fabricated by MCVD and solution doping. The diameter of the core and cladding are $10\ \mu\text{m}$ and $130\ \mu\text{m}$, respectively. The cladding absorption coefficient reaches $3.4\ \text{dB/m}$ at $940\ \text{nm}$. The core absorption coefficient is $35\ \text{dB/m}$ at $1535\ \text{nm}$. The laser test results show that the maximum slope efficiency of $1550\ \text{nm}$ laser is 35.5% , and the output power is greater than $2.5\ \text{W}$. This indicates that phosphorus doping has a significant effect on the optical performance of $\text{Er}^{3+}/\text{Yb}^{3+}$ co-doped fiber. The fiber rapid development lays a solid foundation for further research on a $1.5\text{-}\mu\text{m}$ high-power fiber laser.

Key words laser optics; erbium-ytterbium co-doping fiber; $1.5\ \mu\text{m}$ laser; fiber laser; modified chemical vapor deposition

OCIS codes 140.3280; 140.3500; 140.3510; 160.2290; 160.5690